

QCD sum rules as an inverse problem

Hsiang-nan Li and Hiroyuki Umeeda

Institute of Physics, Academia Sinica, Taipei, Taiwan 115, Republic of China

(Dated: July 26, 2021)

We construct QCD sum rules for nonperturbative studies without assuming the uncertain quark-hadron duality for the spectral density on the hadron side. Instead, both resonance and continuum contributions to the spectral density are solved with the perturbative input on the quark side by treating sum rules as an inverse problem. This new formalism does not involve the continuum threshold, does not require the Borel transformation and stability analysis, and can be extended to extract properties of excited states. Taking the two-current correlator as a example, we demonstrate that the series of ρ resonances can emerge in our formalism, and how to determine the decay constants $f_{\rho(770)}(f_{\rho(1450)}, f_{\rho(1700)}, f_{\rho(1900)}) \approx 0.22$ (0.19, 0.14, 0.14) GeV for the masses $m_{\rho(770)}(m_{\rho(1450)}, m_{\rho(1700)}, m_{\rho(1900)}) \approx 0.78$ (1.46, 1.70, 1.90) GeV. We also show that the decay width $\Gamma_{\rho(770)} \approx 0.17$ GeV can be obtained by substituting a Breit-Wigner parametrization for the $\rho(770)$ pole on the hadron side. It is observed that quark condensates of dimensions six on the quark side are crucial for establishing those ρ resonances. Handling the conventional sum rules with the duality assumption as an inverse problem, we find no hint of the ρ excitations, casting doubt on the multiple pole sum rules widely adopted in the literature. The precision of theoretical outcomes can be improved systematically by including higher-order and higher-power corrections on the quark side. Broad applications of this formalism to abundant low energy QCD observables are expected.

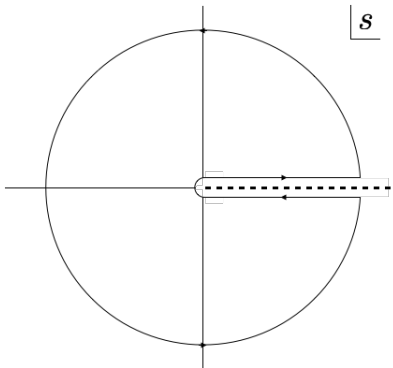
PACS numbers:

I. INTRODUCTION

QCD sum rules have become one of the major nonperturbative approaches to low-energy hadronic processes, since they were proposed decades ago [1]. This approach relies heavily on the assumption of the quark-hadron duality for the spectral density on the hadron side in a low-energy region, whose theoretical uncertainty is difficult to control and quantify. The Borel transformation is applied to suppress model-dependent continuum contributions on the hadron side and higher-power corrections on the quark side. Nevertheless, the typical scale of the Borel mass may not be large enough for justifying the desired suppression sometimes. The choice of the continuum threshold is a bit arbitrary, though the stability criterion, ie., the existence of the so-called "sum rule window", under the variation of the continuum threshold and Borel mass has been imposed. The stability of sum rules may not even exist in some cases (see [2] for example), such that strong dependence on the continuum threshold and Borel mass is not avoidable. Besides, one usually invokes the vacuum saturation hypothesis (factorization) to replace higher-dimension condensates by products of lower-dimension ones on the quark side, which also causes uncertainty. Therefore, there has been concern on the rigorousness and the predictive power of QCD sum rules [3, 4].

In this paper we will construct QCD sum rules without assuming the uncertain quark-hadron duality. The spectral density on the hadron side of a sum rule, including both resonance and continuum contributions, is regarded as an unknown. The operator product expansion (OPE) on the quark side is calculated in the conventional way. A sum rule is then treated as an inverse problem, in which the unknown (source distribution) is solved from the perturbative OPE input (potential observed outside the distribution). This formalism does not involve the continuum threshold, because the continuum can be a smooth distribution not related to the perturbative spectral density. It does not require a Borel transformation to suppress the continuum contribution, which will be solved from the inverse problem. The suppression on the higher power corrections can be achieved by considering the input in the deep euclidean region. Once the unknown spectral density is solved directly, the stability criterion for a conventional sum rule is not necessary. Certainly, the Borel transformation can be applied to our formalism, but it will be verified that results from the versions with and without this transformation are similar.

It has been known that an inverse problem is ill-posed and allows the existence of multiple solutions. We will show that the existence of multiple solutions grants the extension of our formalism to studies of excited states, which imposes a challenge to conventional sum rules. Taking the two-current correlator as a example, we demonstrate how to obtain the masses and decay constants of the ρ resonances. We first fix the correction to the vacuum saturation hypothesis for higher-dimension condensates on the quark side from the input of the ground state $\rho(770)$ mass, and determine the $\rho(770)$ meson decay constant by solving the sum rule as an inverse problem. The lower state observables are then adopted as inputs to extract properties of higher states one by one. That is, a series of (radial) excitations can be probed systematically following the above strategy in our formalism. The masses $m_{\rho(770)}(m_{\rho(1450)}, m_{\rho(1700)}, m_{\rho(1900)}) \approx 0.78$ (1.46, 1.70, 1.90) GeV and the decay constants

FIG. 1: Contour on the complex s plane.

$f_{\rho(770)}(f_{\rho(1450)}, f_{\rho(1700)}, f_{\rho(1900)}) \approx 0.22$ (0.19, 0.14, 0.14) GeV are extracted. We also show that the decay width $\Gamma_{\rho(770)} \approx 0.17$ GeV can be derived by substituting a Breit-Wigner parametrization for the $\rho(770)$ pole on the hadron side. To understand how the nonperturbative condensates influence the appearance of the ρ resonance, we examine the impacts from power corrections of various dimensions. It is found that the quark condensate of dimensions six plays a crucial role for establishing the $\rho(770)$ state.

Properties of excited states have been investigated in the conventional QCD sum rules by employing the double pole plus continuum model for a spectral density [5, 6, 32, 33]. The second pole for the excited state was put in by hand, and ad hoc prescriptions for choosing an appropriate continuum threshold have to be postulated [8], such as the lower bound of the continuum threshold being set to the excited state mass plus 100 MeV. Treating the above convention sum rules as an inverse problem, we explicitly show that the excited ρ resonances do not appear, once the quark-hadron duality is assumed. Our analysis casts doubt on the multiple pole QCD sum rules, which have been widely adopted in the literature. Our formalism is close to the Bayesian approach to QCD sum rules [4], in which the specific form of the spectral density was not assumed either, but derived using the maximum entropy method. Though it is possible to explore the existence of excited states by applying this method to sum rules, at least its application to the nucleon mass spectrum has not been successful [7]. We suspect that the failure is attributed to the ill-posed essence of an inverse problem, which makes difficult searching for correct excitations from infinitely many allowed solutions without any specific parametrization for the spectral density. Hence, our work presents a systematic formalism for studying excited state observables based on QCD sum rules.

In Sec. II we construct our formalism starting from the dispersion relation for a two-current correlator. The distinction from the conventional QCD sum rules, namely, no assumption of the quark-hadron duality, is highlighted. We elaborate the extractions of the masses and decay constants of the series of ρ resonances by solving the sum rules as an inverse problem in Sec. III, starting with the $\rho(770)$ meson mass, which is used to fix the factorization violation parameter κ . The conventional sum rules with the duality assumption are also solved in a similar way to confirm the absence of excited states. Section IV contains the conclusion and outlooks.

II. FORMALISM

The series of ρ resonances is one of the first objects studied in QCD sum rules. In this section we formulate our approach and demonstrate its application, taking these resonances as an example. We first briefly recollect the idea of the conventional QCD sum rules, starting with the two-point correlator

$$\Pi_{\mu\nu}(q^2) = i \int d^4x e^{iq \cdot x} \langle 0 | T[J_\mu(x) J_\nu(0)] | 0 \rangle = (q_\mu q_\nu - g_{\mu\nu} q^2) \Pi(q^2), \quad (1)$$

for the current $J_\mu = (\bar{u}\gamma_\mu u - \bar{d}\gamma_\mu d)/\sqrt{2}$. The vacuum polarization function $\Pi(q^2)$ obeys the identity

$$\Pi(q^2) = \frac{1}{2\pi} \oint ds \frac{\Pi(s)}{s - q^2}, \quad (2)$$

where the contour, depicted in Fig. 1, consists of two pieces of horizontal lines above and below the positive horizontal axis, ie., the branch cut, and a circle of large radius. For s far away from physical poles, the perturbative evaluation

of $\Pi(s)$ is reliable, so the right hand side of Eq. (2) can be written as

$$\frac{1}{2\pi} \oint ds \frac{\Pi(s)}{s - q^2} = \frac{1}{\pi} \int_{s_i}^{\Lambda} ds \frac{\text{Im}\Pi(s)}{s - q^2} + \frac{1}{\pi} \int_{\Lambda}^R ds \frac{\text{Im}\Pi^{\text{pert}}(s)}{s - q^2} + \frac{1}{2\pi} \int_C ds \frac{\Pi^{\text{pert}}(s)}{s - q^2}, \quad (3)$$

where s_i in the first integral denotes the threshold for the nonvanishing spectral density $\text{Im}\Pi(s)$, the numerator in the second integrand has been replaced by the perturbative spectral density $\text{Im}\Pi^{\text{pert}}(s)$ for a sufficiently large separation scale Λ , and C in the third integral represents a large circle of radius R . The spectral density $\text{Im}\Pi(s)$ in the first integrand, involving nonperturbative dynamics from the low s region, will be determined later. The perturbative function $\Pi^{\text{pert}}(s)$ in the third integral receives only the perturbative QCD contribution.

For q^2 in the deep Euclidean region, the perturbative OPE expansion of $\Pi(q^2)$ is reliable, and we have $\Pi^{\text{pert}}(q^2)$ [1] for the left hand side of Eq. (2)

$$\Pi^{\text{pert}}(q^2) = \frac{1}{2\pi} \oint ds \frac{\Pi^{\text{pert}}(s)}{s - q^2} + \frac{1}{12\pi} \frac{\langle \alpha_s G^2 \rangle}{(q^2)^2} + 2 \frac{\langle m_q \bar{q}q \rangle}{(q^2)^2} + \frac{224\pi}{81} \frac{\kappa \alpha_s \langle \bar{q}q \rangle^2}{(q^2)^3}, \quad (4)$$

up to dimension-six condensates, where $\langle G^2 \rangle$ is the gluon condensate, m_q is a quark mass, and the parameter $\kappa = 2-4$ [14–16] is introduced to quantify the violation in the factorization of the four-quark condensate $\langle (\bar{q}q)^2 \rangle$ into the product of $\langle \bar{q}q \rangle$. The first term on the right hand side of the above expression, containing higher order corrections, has been expressed as the contour integral of the perturbative function $\Pi^{\text{pert}}(s)$. The equality of Eq. (3) on the hadron side and Eq. (4) on the quark side leads to

$$\frac{1}{\pi} \int_{s_i}^{\Lambda} ds \frac{\text{Im}\Pi(s)}{s - q^2} = \frac{1}{\pi} \int_{s_i}^{\Lambda} ds \frac{\text{Im}\Pi^{\text{pert}}(s)}{s - q^2} + \frac{1}{12\pi} \frac{\langle \alpha_s G^2 \rangle}{(q^2)^2} + 2 \frac{\langle m_q \bar{q}q \rangle}{(q^2)^2} + \frac{224\pi}{81} \frac{\kappa \alpha_s \langle \bar{q}q \rangle^2}{(q^2)^3}, \quad (5)$$

where the contributions of the perturbative function $\Pi^{\text{pert}}(s)$ in the regions away from physical poles have cancelled from both sides, and only the perturbative spectral density

$$\text{Im}\Pi^{\text{pert}}(q^2) = \frac{1}{4\pi} \left(1 + \frac{\alpha_s}{\pi} \right) \equiv a\pi, \quad (6)$$

along the branch cut remains. Equation (5) is a result of the dispersion relation for the function $\Pi(q^2)$.

The next step is to parametrize the nonperturbative spectral density $\text{Im}\Pi(s)$ on the left hand side of Eq. (5). The translational invariance and the integration over the coordinate x in Eq. (1) gives

$$2\text{Im}\Pi_{\mu\nu}(q^2) = \sum_n \langle 0 | J_\mu | n \rangle \langle n | J_\nu | 0 \rangle d\Phi_n (2\pi)^4 \delta(q - p_n), \quad (7)$$

for $q^2 > 0$, where $d\Phi_n$ and p_n represent the phase space and the momentum of the intermediate state $|n\rangle$, respectively. The ground state for $|n\rangle$ is a neutral vector of the mass m_V and the polarization vector ϵ , which defines the decay constant f_V via the matrix element

$$\langle 0 | J_\mu | V^\lambda \rangle = f_V m_V \epsilon_\mu^\lambda. \quad (8)$$

The substitution of Eq. (8) into Eq. (7) yields

$$\text{Im}\Pi(q^2) = \pi f_V^2 \delta(q^2 - m_V^2) + \pi \rho^h(q^2) \theta(q^2 - s_h), \quad (9)$$

where the first term is a consequence of the narrow width approximation, and the second term denotes the contribution from higher excitations with s_h being their threshold. It has been assumed that the widths of excited states become broader, so their contributions can be parametrized as a continuous spectral density function $\rho^h(q^2)$.

The key of QCD sum rules is the quark-hadron duality, which assumes that the spectral density $\rho^h(q^2)$ is related to the perturbative density $\text{Im}\Pi^{\text{pert}}(q^2)$ as q^2 is higher than some scale $s_0 > s_h$ via

$$\rho^h(s) = \frac{1}{\pi} \text{Im}\Pi^{\text{pert}}(s) \theta(s - s_0), \quad (10)$$

referred to the local duality, or

$$\int_{s_h}^{\Lambda} ds \frac{\rho^h(s)}{s - q^2} = \frac{1}{\pi} \int_{s_0}^{\Lambda} ds \frac{\text{Im}\Pi^{\text{pert}}(s)}{s - q^2}, \quad (11)$$

referred to the global duality. The threshold s_0 is around 1 GeV², so the duality can hardly hold at such a low scale [12, 13]. Obviously, the quark-hadron duality is a major source of theoretical uncertainty, which is not easy to control.

The Borel transformation

$$\hat{B}_M \equiv \lim_{\substack{Q^2, n \rightarrow \infty \\ Q^2/n = M^2}} \frac{1}{(n-1)!} (Q^2)^n \left(-\frac{d}{dQ^2} \right)^n. \quad (12)$$

with $Q^2 \equiv -q^2$, is then employed to suppress the continuum contribution on the hadron side, which has been related to the perturbative spectral density via the duality assumption, and to improve the perturbative OPE expansion on the quark side. Inserting Eqs. (9) and (10) (or (11)) into Eq. (5) under the Borel transformation, we derive the conventional sum rule

$$f_V^2 e^{-m_V^2/M^2} = \frac{1}{\pi} \int_{s_i}^{s_0} ds \text{Im}\Pi^{\text{pert}}(s) e^{-s/M^2} + \frac{1}{12\pi} \frac{\langle \alpha_s G^2 \rangle}{M^2} + 2 \frac{\langle m_q \bar{q}q \rangle}{M^2} - \frac{112\pi}{81} \frac{\kappa \alpha_s \langle \bar{q}q \rangle^2}{M^4}. \quad (13)$$

The prescription for a sum rule calculation is to tune the threshold s_0 in the above formula, such that the value of f_V is stable against the variation of the Borel mass M in a maximal window of M . This prescription introduces theoretical uncertainty, especially when the stability window does not exist [2] as pointed out in the Introduction.

An alternative interpretation of the equality of the hadron and quark sides, in Eq. (5) is that there exist multiple solutions to Eq. (2): the right hand side of Eq. (3), which contains the nonperturbative spectral density $\text{Im}\Pi(s)$ in the first term, can be regarded as a nonperturbative solution to Eq. (2), while the right hand side of Eq. (3) can be regarded as a perturbative solution. Motivated by the above viewpoint, we propose to handle QCD sum rules as an inverse problem, for which multiple solutions exist naturally. First, the spectral density is written as the superposition of the pole and continuum contributions

$$\text{Im}\Pi(q^2) = \pi f_V^2 \delta(q^2 - m_V^2) + \pi \rho^h(q^2), \quad (14)$$

where the threshold s_h for the latter in Eq. (9) does not appear. In fact, the transition from the resonance to continuum region should be smooth, and s_0 in the conventional sum rules is just introduced to characterize the continuum region. Hence, the second term in Eq. (14) behaves like a ramp function [37], taking a value as $q^2 > s_i$, instead of a step function. The unknown function $\pi \rho^h(q^2)$ can be approximated by the perturbative spectral density $\text{Im}\Pi^{\text{pert}}(q^2)$ reliably as q^2 is great than some large separation scale Λ as stated before.

Inserting Eq. (14) into the left hand side of Eq. (5), we write

$$\begin{aligned} \frac{f_V^2}{m_V^2 - q^2} + \int_0^\Lambda ds \frac{\rho^h(s)}{s - q^2} &= \omega(q^2), \\ \omega(q^2) &= a \ln \frac{q^2 - \Lambda}{q^2} + \frac{1}{12\pi} \frac{\langle \alpha_s G^2 \rangle}{(q^2)^2} + 2 \frac{\langle m_q \bar{q}q \rangle}{(q^2)^2} + \frac{224\pi}{81} \frac{\kappa \alpha_s \langle \bar{q}q \rangle^2}{(q^2)^3} \end{aligned} \quad (15)$$

where the threshold $s_i = 4m_\pi^2$ with the pion mass m_π has been set to zero, and the perturbative input $\omega(q^2)$, equal to the right hand side of Eq. (5), is calculable as a standard OPE. The sum rule is then turned into an inverse problem, where the unknowns m_V , f_V and $\rho^h(s)$ are solved with the perturbative input $\omega(q^2)$. We stress that the quark-hadron duality, either Eqs. (10) or (11), is not assumed in the above formalism. It is trivial to apply the Borel transformation to Eq. (15), and we get

$$\begin{aligned} \frac{f_V^2}{M^2} e^{-m_V^2/M^2} + \frac{1}{M^2} \int_0^\Lambda ds \rho^h(s) e^{-s/M^2} &= \hat{\omega}(M^2), \\ \hat{\omega}(M^2) = \hat{B}_M \omega(q^2) &= a(1 - e^{-\Lambda/M^2}) + \frac{1}{12\pi} \frac{\langle \alpha_s G^2 \rangle}{(M^2)^2} + 2 \frac{\langle m_q \bar{q}q \rangle}{(M^2)^2} - \frac{112\pi}{81} \frac{\kappa \alpha_s \langle \bar{q}q \rangle^2}{(M^2)^3}. \end{aligned} \quad (16)$$

It is seen that the suppression on the higher power corrections with the typical $M \sim O(1)$ GeV and by the additional factors $1/(k-1)!$ for the $1/(q^2)^k$ term with $k \leq 3$ is not effective actually. The suppression on the uncertain continuum contribution is not necessary, because it will be solved directly in the present formalism. The suppression on the higher power corrections can be achieved by considering the input $\omega(q^2)$ at large $|q^2|$. As demonstrated in the next section, both versions, Eqs. (15) and (16), lead to similar results for the unknowns. Therefore, we claim that the Borel transformation is not crucial for the new formalism.

To facilitate the numerical analysis, we expand the spectral function $\rho^h(y) \equiv \rho^h(s = y\Lambda)$ in Eq. (15) in a series of Legendre polynomials

$$\rho^h(y) = b_0 P_0(2y - 1) + b_1 P_1(2y - 1) + b_2 P_2(2y - 1) + b_3 P_3(2y - 1) + \cdots, \quad (17)$$

with

$$P_0(y) = 1, \quad P_1(y) = y, \quad P_2(y) = \frac{1}{2}(3y^2 - 1), \quad P_3(y) = \frac{1}{2}(5y^3 - 3y). \quad (18)$$

Other bases of orthogonal functions can serve the purpose equally well. The boundary conditions $\rho^h(0) = 0$ and $\rho^h(1) = a$ impose the constraints

$$b_2 = \frac{a}{2} - b_0, \quad b_3 = \frac{a}{2} - b_1. \quad (19)$$

It will be verified that the expansion up to $P_3(y)$, with the quickly converging coefficients b_i , is sufficient. We will solve Eq. (15) by minimizing the difference between its two sides through tuning Λ , m_V , f_V , b_0 and b_1 .

III. APPLICATION

In this section we extract the observables associated with the series of ρ resonances from our formalism. It is notoriously difficult to solve a Fredholm integral equation like Eq. (15). We have found that the best fit method may be the most transparent way to explore multiple solutions of a Fredholm equation, which has been applied to the explanation of the D meson mixing parameters [10] and the determination of the hadronic vacuum polarization contribution to the muon anomalous magnetic moment [11]. We adopt the following OPE parameters [23, 26] and the running strong coupling evaluated at the scale of 1 GeV

$$\begin{aligned} \Lambda_{\text{QCD}} &= 0.353 \text{ GeV}, \quad \langle m_q \bar{q} q \rangle = 0.007 \times (-0.246)^3 \text{ GeV}^4, \quad \langle \alpha_s G G \rangle = 0.07 \text{ GeV}^4, \\ \alpha_s \langle \bar{q} q \rangle^2 &= 1.49 \times 10^{-4} \text{ GeV}^6, \quad \alpha_s = 0.5. \end{aligned} \quad (20)$$

We consider the input $\omega(q^2)$ from an appropriate range of q^2 in the Euclidean region, in which 20 points q_i^2 are selected, and then search for the set of parameters Λ , m_V , f_V , b_0 and b_1 that minimizes the residual sum of square (RSS)

$$\sum_{i=1}^{20} \left| \frac{f_V^2}{m_V^2 - q_i^2} + \int_0^\Lambda ds \frac{\rho^h(s)}{s - q_i^2} - \omega(q_i^2) \right|^2. \quad (21)$$

Such a set of parameters corresponds to a solution of the Fredholm equation (15). A similar RSS can be defined for the sum rule in Eq. (16) under the Borel transformation, for which the input $\hat{\omega}(M^2)$ is selected from an appropriate range of $M^2 > 0$. We have tested the number of input points from 20 to 500, and confirmed that solutions do not alter with this number.

A. Ground State

The scanning over all the free parameters reveals the minima of the RSS defined in Eq. (21). We present the distributions of the RSS minima on the Λ - m_V planes in Fig. 2 and on the Λ - f_V planes in Fig. 3, where each array contains three columns of plots for $\kappa = 2, 3$, and 4, and three rows for the perturbative inputs from the ranges $(-100 \text{ GeV}^2, -1 \text{ GeV}^2)$ in q^2 , $(-100 \text{ GeV}^2, -10 \text{ GeV}^2)$ in q^2 , and $(1 \text{ GeV}^2, 100 \text{ GeV}^2)$ in M^2 . Nontrivial structures of the RSS minima are observed, which imply the resonance masses m_V and the decay constants f_V preferred by the sum rule in Eq. (15) or (16). A point on a curve of deep color, having RSS about 10^{-14} (10^{-18}) relative to 10^{-8} (10^{-10}) from outside the curve in the first and third (second) row, represents an approximate solution to the sum rules. A solution in the section of the curve with deeper color is closer to the exact solution, and the finite length of this section hints the existence of multiple solutions. A value of Λ signifies the scale, at which the nonperturbative continuum contribution starts to deviate from the perturbative input, so its variation affects the solutions of m_V and f_V . This explains the dependence of the preferred m_V and f_V on Λ , described by the minimum distributions.

It is expected that the power corrections would be enhanced with the input range $(-100 \text{ GeV}^2, -1 \text{ GeV}^2)$ in q^2 compared to $(-100 \text{ GeV}^2, -10 \text{ GeV}^2)$, because the former covers the low Q^2 region. This enhancement is reflected

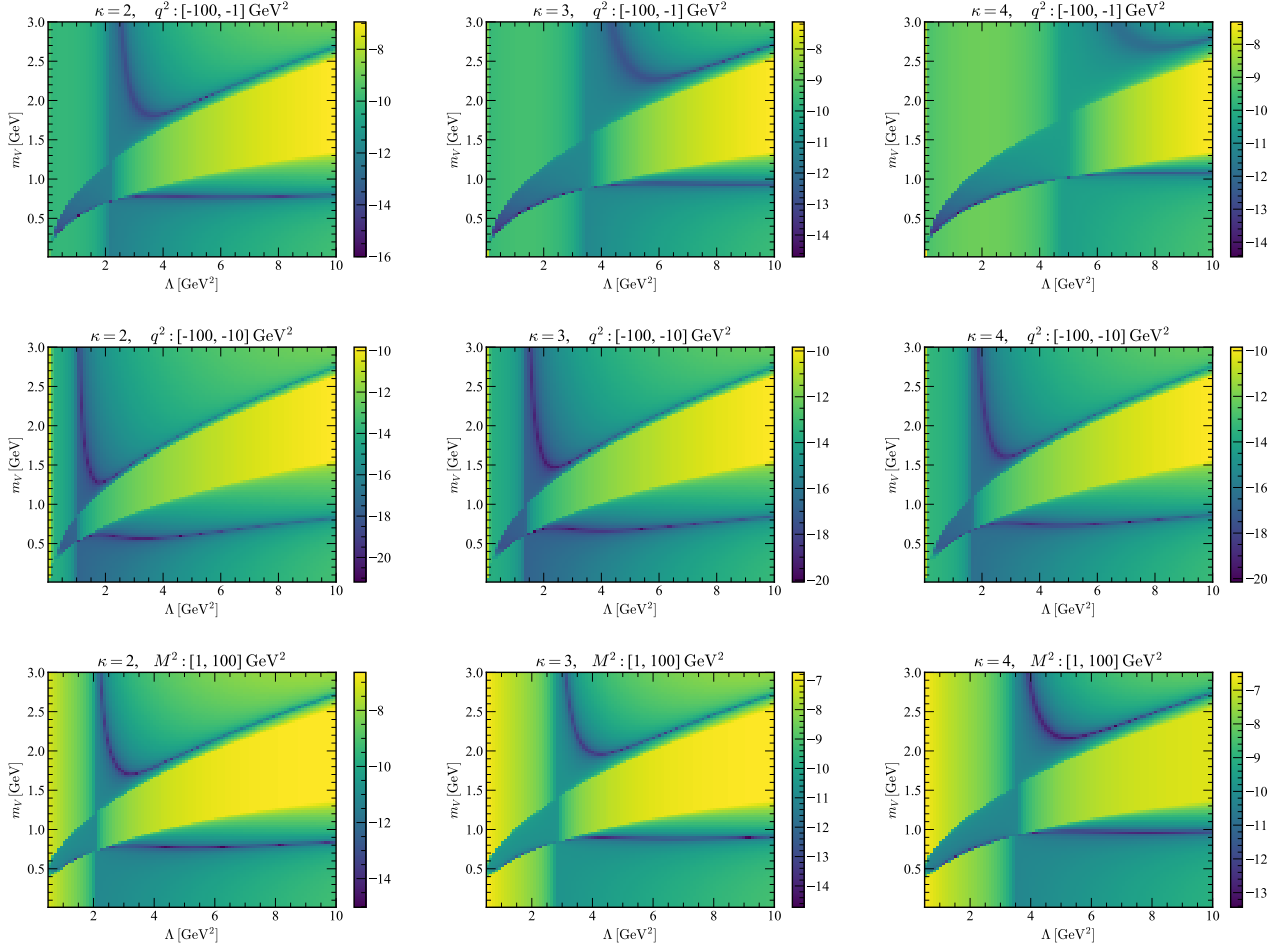


FIG. 2: Minimum distributions of RSS defined in Eq. (21) on the Λ - m_V planes for $\kappa = 2, 3$, and 4 with the input ranges $(-100 \text{ GeV}^2, -1 \text{ GeV}^2)$ in q^2 , $(-100 \text{ GeV}^2, -10 \text{ GeV}^2)$ in q^2 , and $(1 \text{ GeV}^2, 100 \text{ GeV}^2)$ in M^2 .

by the sensitivity of the RSS minimum distributions to the variation of κ in the first row of plots stronger than in the second row. The dependence of the minimum distributions on κ is also more obvious in the third row with the input from low M^2 . Note that the dimension-six four-quark condensate correction becomes comparable to the dimension-four gluon condensate correction, both being of order of 10^{-3} , at Q^2 and M^2 as low as $O(1) \text{ GeV}^2$. The minimum distributions obtained from Eq. (16) with the input range $(1 \text{ GeV}^2, 100 \text{ GeV}^2)$ of M^2 are similar to those from Eq. (15), but exhibit more uniform depth of color. This similarity supports the equivalence of Eqs. (15) and (16), and our postulation that the Borel transformation is not needed, once sum rules are treated as an inverse problem. We will focus only on the analysis of Eq. (15) from now on. As to the input range, we should select the one, where the perturbative term is relatively more important than the condensate corrections, and the OPE is sufficiently convergent. Therefore, we will pick up the input range $(-100 \text{ GeV}^2, -10 \text{ GeV}^2)$ in q^2 for the numerical analysis. We have checked that the input range $(-100 \text{ GeV}^2, -5 \text{ GeV}^2)$ in q^2 leads to the minimum distributions on the Λ - m_V and Λ - f_V planes almost the same as in the middle rows of Figs. 2 and 3, respectively.

It is interesting to see that two minimum distributions appear in the Λ - m_V planes with a gap between them, and the lower ones, being roughly flat (independent of Λ), are located around $m_V \approx 0.8 \text{ GeV}$, which is close to the $\rho(770)$ meson mass $m_{\rho(770)}$. A hadronic resonance is usually built into conventional sum rules through the parametrization in Eq. (9) with the resonance mass being set to the physical value. It has been claimed, based on a stable analytic extrapolation [25], that the present perturbative amplitude in the deep Euclidean region produces a prominent bump structure in the resonance region. Here we have clearly shown that the ground state $\rho(770)$ is predicted by our formalism. The depth of color in the second row of Fig. 2 indicates that global minima along the lower distributions appear in the range $2 \text{ GeV}^2 < \Lambda < 4 \text{ GeV}^2$. We emphasize that the minimum distribution curve in the central plot of Fig. 2 is quite flat, up to $\Lambda = 6 \text{ GeV}^2$, a behavior which can be regarded as kind of stability. The predicted $\rho(770)$

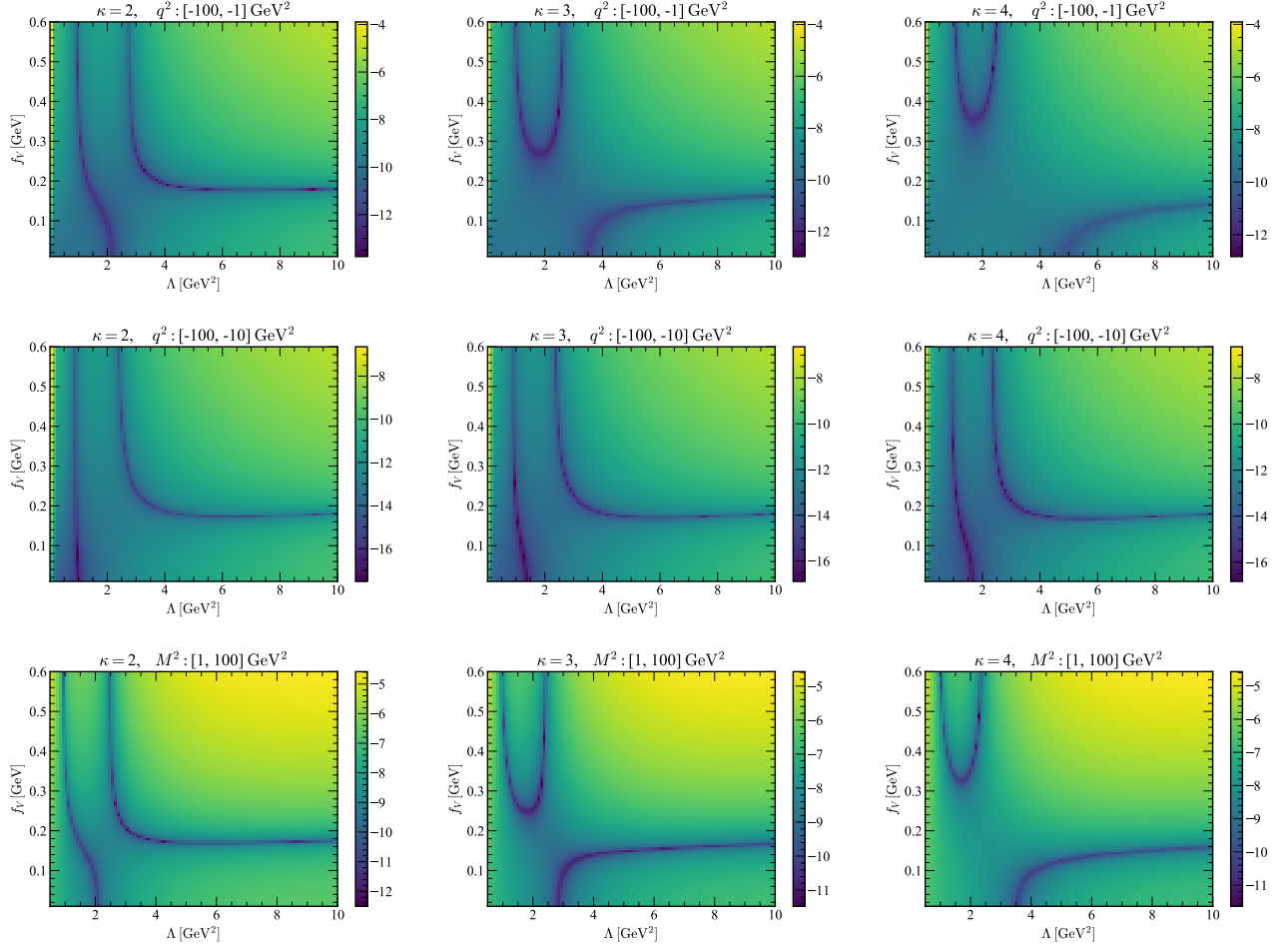


FIG. 3: Minimum distributions of RSS defined in Eq. (21) on the Λ - f_V planes for $\kappa = 2, 3$, and 4 with the input ranges $(-100 \text{ GeV}^2, -1 \text{ GeV}^2)$ in q^2 , $(-100 \text{ GeV}^2, -10 \text{ GeV}^2)$ in q^2 , and $(1 \text{ GeV}^2, 100 \text{ GeV}^2)$ in M^2 .

meson mass read off from the above range is not sensitive to the parameter κ : it varies by about 10% when κ changes from 3 to 4, consistent with what was observed in [23]. The upper minimum distributions in the Λ - m_V plots imply that the single pole parametrization in Eq. (14) allows a larger m_V to be a solution to Eq. (15). We conjecture that the upper distributions are associated with excited states, whose significance will be elaborated in the next subsection.

There is only a single RSS minimum distribution on each Λ - f_V plane in Fig. 3. This is understandable, if the ground state and the first excited state had similar decay constant. The plots in the second row imply a weaker dependence of the minimum distributions on Λ , which are located around $f_V \approx 0.2 \text{ GeV}$, close to the decay constant of the $\rho(770)$ meson. In particular, the second row of Fig. 3 reveals global minima in the range $2 \text{ GeV}^2 < \Lambda < 4 \text{ GeV}^2$, the same as in the second row of Fig. 2. This consistency hints that the best solution to the sum rule in Eq. (15) can accommodate the physical values of the $\rho(770)$ mass and decay constant simultaneously.

We first fix the factorization violation parameter κ associated with the four-quark condensate using the $\rho(770)$ meson mass $m_{\rho(770)} = 0.78 \text{ GeV}$, and adopt this κ value for further analyses. It is easy to find that the mass $m_{\rho(770)} = 0.78 \text{ GeV}$ can be produced with $\kappa = 3.2$, a value also preferred by [16], in a wide range $2 \text{ GeV}^2 < \Lambda < 6 \text{ GeV}^2$ as shown in Fig. 4(a). Since we have ensured that both the best fitted m_V and f_V occur roughly in the same range of Λ , we determine f_V in a less ambiguous way by setting m_V to $m_{\rho(770)} = 0.78 \text{ GeV}$. The resultant Λ - f_V plots from Eq. (15) with the input range $(-100 \text{ GeV}^2, -10 \text{ GeV}^2)$ in q^2 and from Eq. (16) with the input range $(10 \text{ GeV}^2, 100 \text{ GeV}^2)$ in M^2 are displayed in Figs. 4(b) and 4(c), respectively. The global minimum located at $\Lambda = 2.8 \text{ GeV}^2$ on the L-shape minimum distribution in Fig. 4(b) corresponds to the decay constant $f_{\rho(770)} = 0.22 \text{ GeV}$. The separation scale $\Lambda = 2.8 \text{ GeV}^2$ is supposed to be large enough for justifying the replacement of $\text{Im}\Pi(s)$ by $\text{Im}\Pi^{\text{pert}}(s)$ in Eq. (3). A similar value of $f_{\rho(770)}$ is read off from the global minimum located at $\Lambda = 2 \text{ GeV}^2$ in Fig. 4(c), confirming the equivalence between Eqs. (15) and (16). The above results of $m_{\rho(770)}$ and $f_{\rho(770)}$ agree with those in

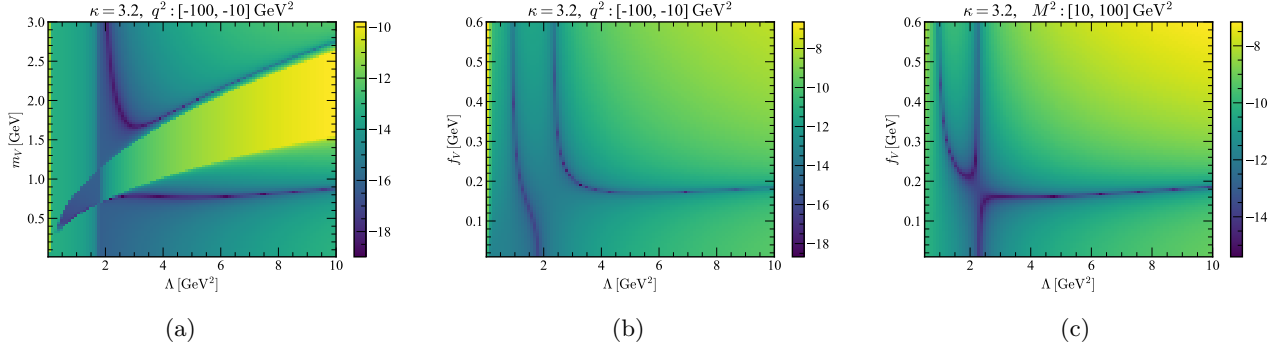


FIG. 4: Minimum distributions of RSS (a) on the Λ - m_V plane for $\kappa = 3.2$ with the input range $(-100 \text{ GeV}^2, -10 \text{ GeV}^2)$ in q^2 (left), (b) on the Λ - f_V with m_V being further set to $m_{\rho(770)} = 0.78 \text{ GeV}$, and (c) on the Λ - f_V plane for $\kappa = 3.2$ and $m_V = 0.78 \text{ GeV}$ with the input range $(10 \text{ GeV}^2, 100 \text{ GeV}^2)$ in M^2 .

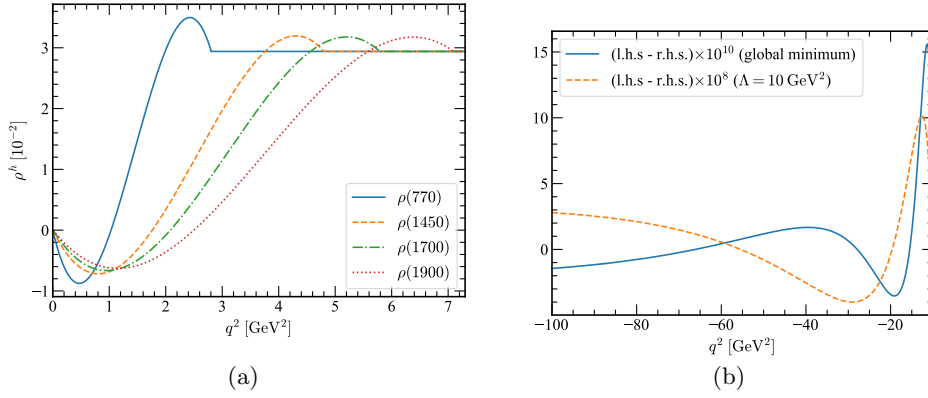


FIG. 5: (a) behavior of the spectral function $\rho^h(q^2)$ in q^2 , and (b) difference between the two sides of Eq. (15) for the best fit solution in Fig. 4(b), and a solution on the minimum distribution located at $\Lambda = 10 \text{ GeV}^2$.

[9], from the lattice calculation [17], from the Bethe-Salpeter equation [19–21], and from the light-front quark model [18].

We also read off the coefficients in the expansion of the spectral function $\rho^h(q^2)$ in terms of the Legendre polynomials, which correspond to the selected global minimum located at $\Lambda = 2.8 \text{ GeV}^2$ in Fig. 4(b):

$$b_0 = 0.0126, \quad b_1 = 0.0276, \quad b_2 = 0.0022, \quad b_3 = -0.0128. \quad (22)$$

If two more Legendre polynomials are included in the expansion, the global minimum shifts to $\Lambda = 3.1 \text{ GeV}^2$ with the corresponding decay constant $f_\rho = 0.23 \text{ GeV}$, and we get

$$b_0 = 0.0120, \quad b_1 = 0.0308, \quad b_2 = -0.0040, \quad b_3 = -0.0202, \quad b_4 = 0.0068, \quad b_5 = 0.0042. \quad (23)$$

The stability of the coefficients b_0, \dots, b_3 and the smallness of b_4 and b_5 verify that the expansion up to the P_3 term is enough. The behavior of $\rho^h(q^2)$ in q^2 for Eq. (22) is depicted in Fig. 5(a), which differs dramatically from the step function in Eq. (10) based on the local quark-hadron duality. Note that the slope of the solved $\rho^h(q^2)$ is discontinuous at $q^2 = \Lambda = 2.8 \text{ GeV}^2$, where it transits to the perturbative spectra function, because we have not yet imposed the continuity constraint to the slope. The function $\rho^h(q^2)$ is slightly negative at q^2 , where the pole is located. This negative contribution is expected to be compensated by that from the resonance, when its finite width is taken into account.

We compare the q^2 dependencies of the left hand side from the best fit solution and of the right hand side of Eq. (15) by showing their difference in Fig. 5(b). For the purpose of comparison, we select a solution on the minimum distribution located at $\Lambda = 10 \text{ GeV}^2$, far away from the global minimum, in the Fig. 4(b), which corresponds to $f_V = 0.18 \text{ GeV}$, and show the difference between the two sides of Eq. (15). It is obvious that the two sides of Eq. (15) match each other well in the former case, and that the difference between the two sides is about 100 times larger in the latter case.

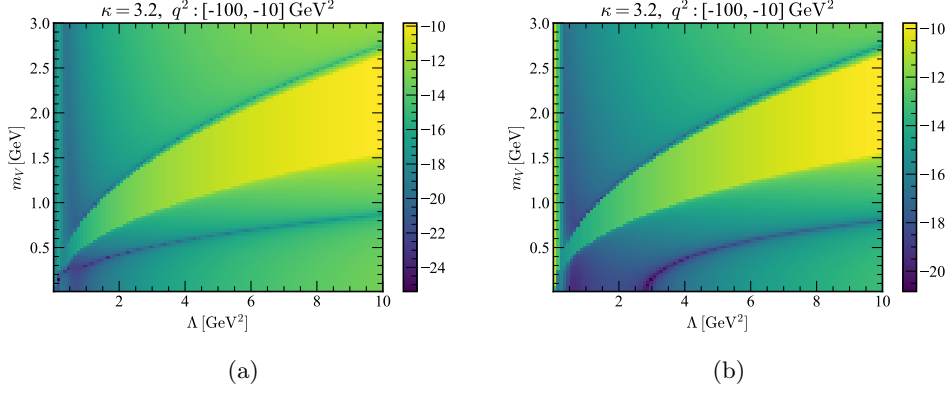


FIG. 6: Minimum distributions of RSS on the Λ - m_V planes for $\kappa = 3.2$ with the input of (a) the perturbative piece only range, and (b) without the $1/(q^2)^3$ power correction from the range $(-100 \text{ GeV}^2, -10 \text{ GeV}^2)$ of q^2 .

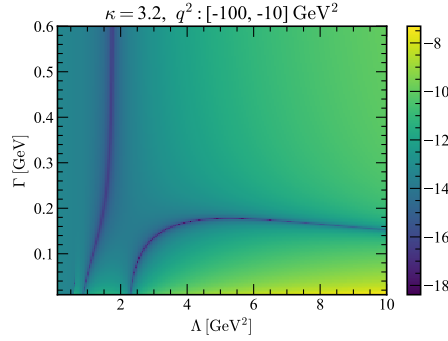


FIG. 7: Minimum distribution of RSS on the Λ - Γ plane for $\kappa = 3.2$ with the input from the range $(-100 \text{ GeV}^2, -10 \text{ GeV}^2)$ of q^2 .

Next we investigate how each term in the OPE input influences the emergence of the ρ resonances in Fig. 2. The RSS minimum distributions on the Λ - m_V plane for the two cases, with only the perturbative piece and without the $1/(q^2)^3$ power correction, are presented in Figs. 6(a) and 6(b), respectively. It is seen that the two minimum distributions have very light color in the former, and both grow with Λ without a stable region. It implies that the perturbative piece alone does not induce a bound state. When the $1/(q^2)^2$ terms, ie., the gluon and two-quark condensates, are turned on, the lower minimum distribution in Fig. 6(b) gets enhanced and shifts toward the larger Λ region, but still does not exhibit a stable value of m_V . The upper minimum distribution remains as dim as in Fig. 6(a). When all the terms on the right hand sides of Eq. (15) are present, the stable ground state mass appears, and the upper minimum distribution also gets enhanced as shown in Fig. 4. The observation is that all the terms in the OPE work together to generate the ρ resonance, and the four-quark condensate is more crucial for its emergence.

Below we extract the ρ meson decay width from our formalism by inserting the $\pi^+\pi^-$ state and other multi-hadron states into the correlator in Eq. (1), among which the matrix element $\langle 0|J_\mu|\pi^+\pi^- \rangle$ defines the time-like pion form factor. The ρ resonance contributes to the spectral density dominantly, which is parametrized as [22, 23]

$$\text{Im}\Pi(q^2) = \frac{1}{24\pi} \frac{m_V^4 + m_V^2\Gamma^2}{(q^2 - m_V^2)^2 + m_V^2\Gamma^2} + \pi\rho^h(q^2). \quad (24)$$

with the decay width Γ . The first term in the above expression corresponds to the time-like pion form factor, which describes the decay of a ρ meson, produced in the e^+e^- annihilation, into a pion pair. No three pion states are involved here, which arise from the ω resonance suppressed by the isospin-1 current. One should be reminded that the boundary conditions $\rho^h(0) = 0$ and $\rho^h(1) = a$ will be modified into $\text{Im}\Pi(0) = 0$ and $\text{Im}\Pi(\Lambda) = a\pi$. We set $m_V = m_\rho$, and analyze the minimum distribution on the $\Lambda - \Gamma$ plane, which is shown in Fig. 7. We have tested other parametrizations for the time-like pion form factor, such as the one in [24], and similar minimum distributions are obtained. It is noticed that the global minimum located at $\lambda = 4.3 \text{ GeV}^2$ gives $\Gamma = 0.17 \text{ GeV}$, close to the value in [9]. We mention that it is difficult to reproduce the width of the $\rho(770)$ meson with any reasonable precision in

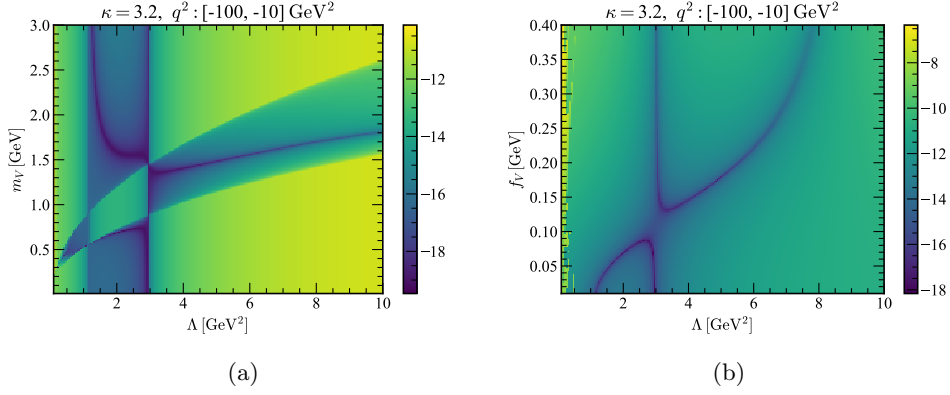


FIG. 8: Minimum distributions of RSS (a) on the Λ - m_V plane in the double pole parametrization for $\kappa = 3.2$ with the input range $(-100 \text{ GeV}^2, -10 \text{ GeV}^2)$ in q^2 , and (b) on the Λ - f_V plane with m_V being further set to $m_{\rho'} = 1.46 \text{ GeV}$.

the Bayesian approach [4], because of the insufficient sensitivity of the detailed $\rho(770)$ peak form to the perturbative input.

B. Excited States

The upper minimum distributions on the Λ - m_V planes in Fig. 2, with a gap above the lower ones, hint strongly that other resonances exist, though a single pole parametrization for the spectral density was adopted in Eq. (14). Combining the implication of the Λ - f_V plots in Fig. 3, we speculate that an excited ρ state with the decay constant around 0.2 GeV can also satisfy the sum rule in Eq. (15). Compared to the lower minimum distributions, referred to the ground state $\rho(770)$, the minimum distributions associated with excited states exhibit more significant sensitivity to the variation of the separation scale Λ . This is understandable, because more excited states, which are denser in the mass spectrum, will be covered as Λ increases, such that a single pole parametrization becomes more improper. To study properties of an excited state, we modify the spectral density in Eq. (14) into

$$\text{Im}\Pi(q^2) = \pi f_{\rho(770)}^2 \delta(q^2 - m_{\rho(770)}^2) + \pi f_V^2 \delta(q^2 - m_V^2) + \pi \rho^h(q^2), \quad (25)$$

where the ground state mass and decay constant have been set to $m_{\rho(770)} = 0.78 \text{ GeV}$ and $f_{\rho(770)} = 0.22 \text{ GeV}$ determined in the previous subsection. That is, the first excited state has been moved out of the continuum and treated as the second isolated resonance in the above parametrization. Certainly, the RSS definition in Eq. (21) is also modified accordingly with two resonance terms being included.

We observe the RSS minimum distribution on the Λ - m_V plane with the OPE input range $(-100 \text{ GeV}^2, -10 \text{ GeV}^2)$ in q^2 and $\kappa = 3.2$ in Fig. 8(a). Given the mass and decay constant of the $\rho(770)$ meson in Eq. (25), the minimum distribution indeed becomes less Λ dependent at large Λ , compared to the upper minimum distribution in Fig. 4(a). In particular, global minima in the range $\Lambda \approx 3$ -5 GeV^2 imply the preferred values of m_V around 1.5 GeV, close to the $\rho(1450)$ meson mass $m_{\rho(1450)} = 1.46 \text{ GeV}$. That is, we have found the indication for the existence of the first excited ρ state in our formalism. A seeming U-shape minimum distribution attaches to the tilted one without a gap, a layout quite different from Fig. 4(a). Note that there may exist another state $\rho(1570)$ with the similar mass, that has been speculated to be due to an OZI-suppressed decay mode of $\rho(1700)$ [9]. It is not clear whether the gapless minimum distribution is related to these two nearby states $\rho(1450)$ and $\rho(1570)$. A more precise OPE input may be needed to clarify this issue.

We then choose m_V as $m_{\rho(1450)} = 1.46 \text{ GeV}$, namely, fix the considered excited state to be $\rho(1450)$, and find the minimum distribution on the Λ - f_V plane. We discard the distribution in the low Λ region in Fig. 8(b), because the separation scale should be higher than $m_{\rho(1450)}^2$ to search for a physical solution of the two pole parametrization in Eq. (25). The preferred $f_{\rho(1450)} = 0.19 \text{ GeV}$ is read off from the global minimum located at $\Lambda = 4.8 \text{ GeV}^2$. The value $f_{\rho(1450)} = 0.19 \text{ GeV}$ leads to the ratio of the two τ decay widths,

$$\frac{\Gamma(\tau \rightarrow \rho(1450)\nu_\tau)}{\Gamma(\tau \rightarrow \rho(770)\nu_\tau)} = \frac{(m_\tau^2 - m_{\rho(1450)}^2)f_{\rho(1450)}^2}{(m_\tau^2 - m_{\rho(770)}^2)f_{\rho(770)}^2} \approx 0.3. \quad (26)$$

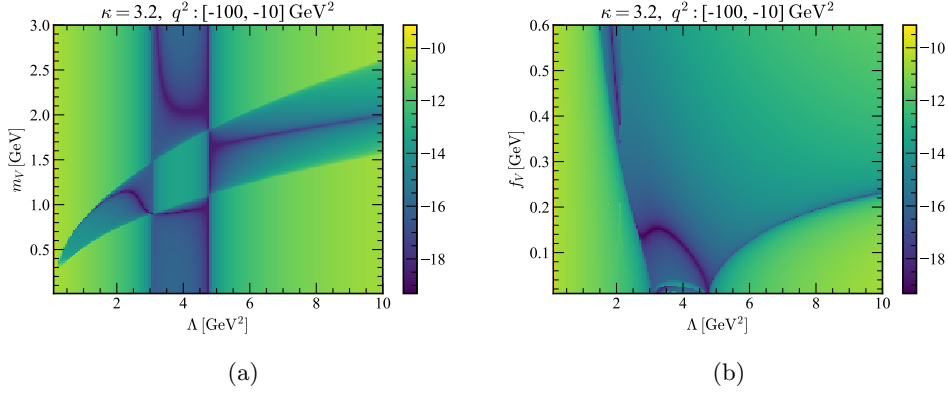


FIG. 9: Minimum distributions of RSS (a) on the Λ - m_V plane in the triple pole parametrization for $\kappa = 3.2$ with the input range $(-100 \text{ GeV}^2, -10 \text{ GeV}^2)$ in q^2 , and (b) on the Λ - f_V plane with m_V being further set to $m_{\rho(1700)} = 1.70 \text{ GeV}$.

for the masses $m_\tau = 1.777 \text{ GeV}$, $m_{\rho(770)} = 0.775 \text{ GeV}$ and $m_{\rho(1450)} = 1.465 \text{ GeV}$, and the decay constant $f_{\rho(770)} = 0.22 \text{ GeV}$. The above ratio, being larger than the estimate 0.1 in the extended Nambu-Jona-Lasinio model [27], can be confronted with future data.

We point out that the continuum contribution to the spectral density differs from the one described by Eq. (22), because the first excited state $\rho(1450)$ has been moved out of the continuum. The coefficients of the Legendre polynomials corresponding to the global minimum in Fig. 8(b) are modified into

$$b_0 = 0.0104, \quad b_1 = 0.0248, \quad b_2 = 0.0033, \quad b_3 = -0.0101. \quad (27)$$

so the expansion of the spectral density function up to the P_3 term is still enough. The behavior of the spectral density function $\rho^h(q^2)$ in q^2 is displayed in Fig. 5(a), which differs from the step function in Eq. (10) and from the one associated with the single pole solution. It is natural that $\rho^h(q^2)$ becomes sizable at higher q^2 , when more resonances are moved out of the continuum. The above observation makes clear the key improvement in our formalism compared to the conventional sum rules: properties of excited states can be explored in sum rules by solving them as an inverse problem, instead of assuming the quark-hadron duality for a spectral density. Without the duality assumption, there is more freedom to adjust the continuum contribution according to considered resonances.

The strategy to extract the observables associated with the next excited state is clear now in our formalism. The study of higher excited states is expected to be more difficult, because they become denser in the mass spectrum. Motivated by the appearance of the additional U-shape minimum distribution on the Λ - m_V plane in Fig. 9(a), we repeat the procedure. To examine whether there are higher excited states, we further modify the spectral density into

$$\text{Im}\Pi(q^2) = \pi f_{\rho(770)}^2 \delta(q^2 - m_{\rho(770)}^2) + \pi f_{\rho(1450)}^2 \delta(q^2 - m_{\rho(1450)}^2) + \pi f_V^2 \delta(q^2 - m_V^2) + \pi \rho^h(q^2), \quad (28)$$

where the mass and the decay constant of the $\rho(1450)$ meson have been set to $m_{\rho(1450)} = 1.46 \text{ GeV}$ and $f_{\rho(1450)} = 0.19 \text{ GeV}$ derived before, respectively. The RSS minimum distribution on the Λ - m_V plane with the OPE input range $(-100 \text{ GeV}^2, -10 \text{ GeV}^2)$ in q^2 and $\kappa = 3.2$ is presented in Fig. 9(a). The U-shape minimum distribution appears again, but with a gap above the slightly tilted one. It is easy to find the global minima located on the tilted minimum distribution around $\Lambda \sim 5 \text{ GeV}^2$, which corresponds to $m_V \approx 1.7 \text{ GeV}$, exactly the $\rho(1700)$ meson mass [9]. That is, the second excited ρ state also emerges in our formalism.

We then search the minimum distribution on the Λ - f_V plane with m_V being set to the value of $m_{\rho(1700)} = 1.7 \text{ GeV}$, namely, with the considered excited state being fixed to $\rho(1700)$. The minimum distribution, displayed in Fig. 9(b), also reveals a nontrivial structure. We read off the decay constant $f_{\rho(1700)} = 0.14 \text{ GeV}$ from the global minimum located at $\Lambda = 5.8 \text{ GeV}^2$. The associated coefficients in the polynomial expansion are modified into

$$b_0 = 0.0106, \quad b_1 = 0.0244, \quad b_2 = 0.0031, \quad b_3 = -0.0099, \quad (29)$$

and the resultant behavior of the spectral function is displayed in Fig. 5(a). As expected, the spectral density function shifts further toward the large q^2 region with one more excited state being moved out of the continuum.

One may wonder whether even higher excited ρ states, like $\rho(1900)$, can be probed in our formalism, because some nontrivial U-shape minimum distribution still shows up in Fig. 9(a). Adopting the spectral density

$$\text{Im}\Pi(q^2) = \frac{\pi}{2} f_\rho^2 \delta(q^2 - m_\rho^2) + \frac{\pi}{2} f_{\rho(1450)}^2 \delta(q^2 - m_{\rho(1450)}^2) + \frac{\pi}{2} f_{\rho(1700)}^2 \delta(q^2 - m_{\rho(1700)}^2) + \frac{\pi}{2} f_V^2 \delta(q^2 - m_V^2) + \pi \rho^h(q^2) \quad (30)$$

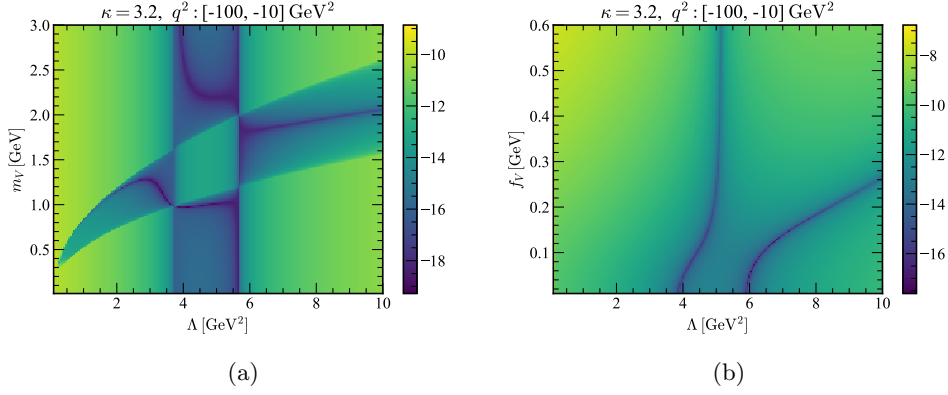


FIG. 10: Minimum distributions of RSS (a) on the Λ - m_V plane in the quadruple pole parametrization for $\kappa = 3.2$ with the input range $(-100 \text{ GeV}^2, -10 \text{ GeV}^2)$ of q^2 , and (b) on the Λ - f_V plane with m_V being further set to $m_{\rho(1900)} = 1.90 \text{ GeV}$.

we analyze the minimum distribution on the Λ - m_V plane shown in Fig. 10(a), where the curve indicates global minima located in the range $\Lambda \sim 6\text{--}7 \text{ GeV}^2$ with $m_V \sim 1.9 \text{ GeV}$. It is exactly the $\rho(1900)$ meson mass [9], implying that the third excited ρ state still emerges in our formalism. We then search the minimum distribution on the Λ - f_V plane with m_V being set to the value of $m_{\rho(1900)} = 1.9 \text{ GeV}$, namely, with the considered excited state being fixed to $\rho(1900)$. The global minimum in Fig. 10(b) located at $\Lambda = 7.1 \text{ GeV}^2$ gives the decay constant $f_{\rho(1900)} = 0.14 \text{ GeV}$, which marks a prediction of our formalism. The corresponding coefficients in the polynomial expansion are

$$b_0 = 0.0118, \quad b_1 = 0.0242, \quad b_2 = 0.0028, \quad b_3 = -0.0095, \quad (31)$$

and the resultant behavior of the spectral density function is exhibited in Fig. 5(a). Though there is a vague U -shape minimum distribution above the tilted one, we will not proceed further the test application, and end the search of the excited ρ states here.

Our results for the decay constants of the excited $\rho(1450)$ and $\rho(1700)$ and resonances are comparable to those derived in the literature, such as the sum rule analysis with nonlocal condensate corrections [5, 6], the double pole QCD sum rules [8], the light cone quark model [34], the lattice QCD [35], and the rainbow-ladder truncation method [36]. The theoretical and experimental studies on the $\rho(1900)$ state are still rare. Our formalism can certainly be applied to extract the decay widths of excited ρ states, which will be published elsewhere with more detailed analyses. At last, we make a remark on the sum rule analysis based on the Maximum Entropy Method. It is unlikely to reveal all the bound states simultaneously, especially when the mass spectrum becomes dense, and when multiple solutions exist for such an inverse problem. It may be possible to explore excited states using this method, if one follows our strategy: find the best-fit solution for excited states one by one. We will validate this conjecture in a future publication.

C. Sum Rules with Duality Assumption

As an alternative viewpoint, an over-simplified model, ie., the duality assumption with a single parameter s_0 , has been employed in conventional sum rules. This simple model satisfies the boundary conditions automatically, because it is a step function: it vanishes at $s = 0$, and the duality assumption guarantees the continuity condition at $s = s_0$. Compared to our polynomial expansion, we have two free parameters actually, b_0 and b_1 . In this sense, our parametrization may be simple too, but it is more general than the duality assumption. We will show that one may not be able to explore properties of the excited states under the duality assumption. For the convenience of discussion below, we present the version of Eq. (13) before the Borel transformation,

$$\frac{f_V^2}{m_V^2 - q^2} = \frac{1}{\pi} \int_{s_i}^{s_0} ds \frac{\text{Im}\Pi^{\text{pert}}(s)}{s - q^2} + \frac{1}{12\pi} \frac{\langle \alpha_s G^2 \rangle}{(q^2)^2} + 2 \frac{\langle m_q \bar{q}q \rangle}{(q^2)^2} + \frac{224\pi}{81} \frac{\kappa \alpha_s \langle \bar{q}q \rangle^2}{(q^2)^3}. \quad (32)$$

The conventional sum rules in Eqs. (13) and (32) can also be handled as an inverse problem with the three unknowns m_V , f_V and s_0 (the lower bounds s_i in the integrals on the right hand sides of Eqs. (32) and (13) have been approximated by zero). For simplicity, we focus only on Eq. (32), and take the power corrections in the range

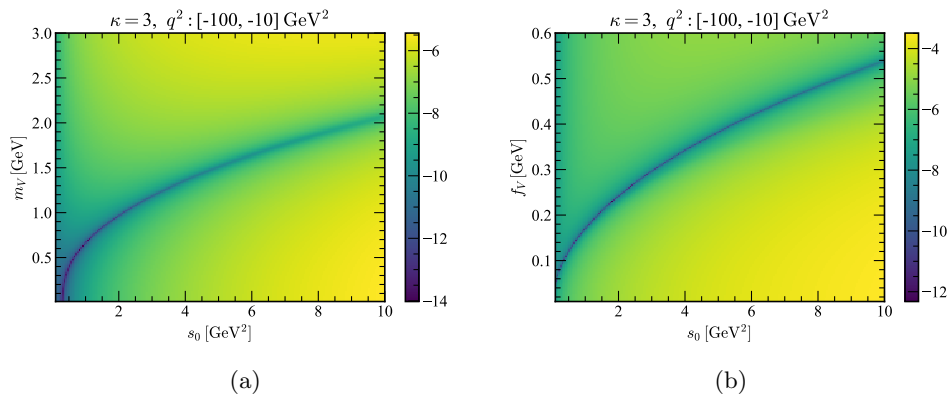


FIG. 11: Minimum distributions of RSS for the conventional sum rules with the duality assumption on (a) the s_0 - m_V plane and (b) the s_0 - f_V plane with $\kappa = 3$ and the input range $(-100 \text{ GeV}^2, -10 \text{ GeV}^2)$ in q^2 .

$(-100 \text{ GeV}^2, -10 \text{ GeV}^2)$ in q^2 as the input. It has been verified that results derived from the sum rule under the Borel transformation in Eq. (13) are the same.

The minimum distributions on the s_0 - m_V and s_0 - f_V planes for $\kappa = 3$ are presented in Fig. 11(a) and (b), respectively. The minimum distributions for $\kappa = 2$ and 4 are similar. It is found that there is only one minimum distribution on the s_0 - m_V , which increases monotonically with s_0 . Note that a plot in Fig. 2 contains two minimum distributions, where the lower one, corresponding to m_V around 0.78 GeV, is stable with respect to the variation of Λ , and the upper one appears with a mass gap. The color of the minimum distribution of RSS is darker for s_0 between 0 and 2 GeV^2 , which covers a wide range of m_V values between 0 and 1 GeV. In particular, neither a global minimum nor a plateau exists at the $\rho(770)$ meson mass. Certainly, one can choose an appropriate s_0 value, say, $s_0 \sim 1.5$ to get $m_V = 0.78$ GeV. Then with this s_0 , one can read off $f_V \sim 0.2$ GeV from Fig. 11(b). In this sense the conventional sum rules are less predictive with uncontrollable uncertainty, but still useful for estimating the decay constant of the ground state, if its mass is fixed. To have a chance of revealing $\rho(1450)$, the curve has to reach 1.45 GeV before s_0 exceeds the upper bound set by the $\rho(1700)$ mass by definition. Obviously, this is not the case as indicated by Fig. 11(a). Besides, the lack of an upper minimum distribution hints the absence of excited states, and does not motivate a pursuit of excited states in conventional sum rules. Therefore, it seems difficult to justify the double pole sum rules widely adopted in the literature.

IV. CONCLUSION

In this paper we have modified QCD sum rules for nonperturbative studies without the assumption of the uncertain quark-hadron duality. The spectral density on the hadron side, including both resonance and continuum contributions, is solved with the perturbative input on the quark side by treating sum rules as an inverse problem. We have elaborated the postulation that the Borel transformation is not crucial for this new formalism, because the continuum contribution needs not to be suppressed, but is solved from the inverse problem, and the convergence of the OPE is achieved by considering the input in the deep euclidean region. Once the unknown spectral density is solved directly, the stability criterion for conventional sum rules is not necessary either. The implementation of the above formalism has been demonstrated by identifying the series of ρ states and by determining their corresponding decay constants from the two-current correlator. The strategy is to include resonances one by one into the spectral density with different associated continuum contributions, and repeat solving the sum rules by minimizing the difference between the hadron and quark sides. One should make sure in the above procedure that the scale Λ , separating the perturbative and nonperturbative regimes, should be above the highest resonance mass parametrized into the unknown spectra density for consistency. In this way we have obtained the decay constants $f_{\rho(770)}(f_{\rho(1450)}, f_{\rho(1700)}, f_{\rho(1900)}) \approx 0.22$ (0.19, 0.14, 0.14) GeV for the masses $m_{\rho(770)}(m_{\rho(1450)}, m_{\rho(1700)}, m_{\rho(1900)}) \approx 0.78$ (1.46, 1.7, 1.9) GeV of the ρ resonances. The decay width $\Gamma_{\rho(770)} \approx 0.17$ GeV of the $\rho(770)$ meson has been also obtained. We mentioned that the existence the $\rho(1570)$ state could not be excluded, which has been speculated to be due to an OZI-suppressed decay mode of $\rho(1700)$.

The major sources of theoretical uncertainties arise from the OPE for the perturbative inputs. First, the OPE is truncated at finite orders in α_s and at finite powers of $1/q^2$. We have speculated that higher power corrections may be needed to establish higher excited states with correct masses. This is the reason we have stopped the search for

excited states at $\rho(1900)$. More precise inputs, such as reliable evaluations of the parameter κ and higher dimension condensates, help determine the values of nonperturbative observables. Here we have fixed κ to be 3.2 to produce the correct $\rho(770)$ meson mass. Second, the expansion of the spectral function $\rho^h(y = s/\Lambda)$ in a series of Legendre polynomials is truncated at the fourth term. Though the convergence of this expansion has been scrutinized, the precision of our predictions can be improved by including higher order polynomials. When this is achieved, the continuity of the slope of the spectral density function at the separation scale can also be imposed. It is claimed that both the above sources of theoretical uncertainties can be reduced straightforwardly and systematically. One may still question whether the separation scales Λ about few GeV^2 in our study are large enough for justifying the replacement of the continuum contribution $\Im\Pi(s)$ by the perturbative one $\Im\Pi^{\text{pert}}(s)$, which is also based on the quark-hadron duality. Certainly, it is not the concerned duality assumption in conventional QCD sum rules around the threshold $s_0 \approx 1 \text{ GeV}^2$, and the duality violation above $\Lambda \approx \text{few GeV}^2$ is expected to be minor.

This new formalism is expected to be more predictive with less ambiguity and more control of theoretical uncertainty, compared to conventional sum rules, because the unknown observables were extracted from global minima. In particular, it can be extended to analyses of excited states, which are difficult to achieve in conventional sum rules. Since whether a bound state exists can be explored in our formalism, it would be of interest to apply it to the various exotic channels, containing more than three quarks. We have observed that the condensate corrections up to dimension 6 seem to sufficient for generating most known ρ resonances, it deserves an investigation how higher dimensional condensates affect the results presented here. Because of the huge uncertainty of the dimension-eight condensate [28–31], it may be unlikely to have a concrete conclusion. It is worthwhile to generalize it to pursue nonperturbative properties of vector mesons in nuclear medium [39] at finite density or temperature to directly observe the change in the spectral function in hot or dense environments. Our formalism cannot only be applied to low energy light flavor processes, but also to heavy flavor physics [40–44]. It is also possible to extend the new formalism to studies of more complicated QCD processes, which need to involve the nonlocal condensate corrections in the OPE [45–48], and of nonlocal condensate effects on excited states [5, 6]. There is no doubt that there are broad applications of our nonperturbative formalism.

Acknowledgement

This work was supported in part by the Ministry of Science and Technology of R.O.C. under Grant No. MOST-107-2119-M-001-035-MY3.

-
- [1] M. A. Shifman, A. I. Vainshtein and V. I. Zakharov, Nucl. Phys. B **147**, 385 (1979); B **147**, 448 (1979).
 - [2] C. Coriano and H. n. Li, Phys. Lett. B **324**, 98 (1994).
 - [3] D. B. Leinweber, Annals Phys. **254**, 328-396 (1997).
 - [4] P. Gubler and M. Oka, Prog. Theor. Phys. **124**, 995-1018 (2010).
 - [5] A. Bakulev and S. Mikhailov, Phys. Lett. B **436**, 351-362 (1998).
 - [6] A. Pimikov, S. Mikhailov and N. Stefanis, Few Body Syst. **55**, 401-406 (2014).
 - [7] K. Ohtani, P. Gubler and M. Oka, Phys. Rev. D **87**, no.3, 034027 (2013).
 - [8] M. Maior de Sousa and R. da Silva, Braz. J. Phys. **46**, no.6, 730-739 (2016).
 - [9] M. Tanabashi *et al.* [Particle Data Group], Phys. Rev. D **98**, no.3, 030001 (2018).
 - [10] H. N. Li, H. Umeeda, F. Xu and F. S. Yu, arXiv:2001.04079 [hep-ph].
 - [11] H. N. Li and H. Umeeda, arXiv:2004.06451 [hep-ph].
 - [12] D. Boito, M. Golterman, M. Jamin, K. Maltman and S. Peris, Phys. Rev. D **87**, no.9, 094008 (2013).
 - [13] M. Gonzalez-Alonso, A. Pich and A. Rodriguez-Snchez, Phys. Rev. D **94**, no.1, 014017 (2016).
 - [14] Y. Chung, H. G. Dosch, M. Kremer and D. Schall, Z. Phys. C **25**, 151 (1984).
 - [15] S. Narison, Phys. Lett. B **361**, 121 (1995).
 - [16] S. Narison, Phys. Lett. B **673**, 30 (2009).
 - [17] W. Sun *et al.* [χ QCD], Chin. Phys. C **42**, no.6, 063102 (2018).
 - [18] H. M. Choi and C. R. Ji, Phys. Rev. D **75**, 034019 (2007).
 - [19] S. Bhatnagar and Shi-Yuan Li, J. Phys. G **32**, 949 (2006).
 - [20] Z. G. Wang and S. L. Wan, Phys. Rev. C **76**, 025207 (2007).
 - [21] M. Blank, A. Krassnigg and A. Maas, Phys. Rev. D **83**, 034020 (2011).
 - [22] C. A. Dominguez and N. Paver, Z. Phys. C **31**, 591 (1986).
 - [23] Q. N. Wang, Z. F. Zhang, T. Steele, H. Y. Jin and Z. R. Huang, Chin. Phys. C **41**, no.7, 074107 (2017).
 - [24] M. Fischer *et al.* [ETM], [arXiv:2006.13805 [hep-lat]].
 - [25] R. Buchert and N. A. Papadopoulos, Phys. Lett. B **296**, 430 (1992).
 - [26] S. Narison, Nucl. Part. Phys. Proc. **258-259**, 189-194 (2015).

- [27] A. Ahmadov, Y. L. Kalinovsky and M. Volkov, *Int. J. Mod. Phys. A* **30**, no.26, 1550161 (2018).
- [28] B. Blok and M. Lublinsky, *Phys. Rev. D* **57**, 2676-2690 (1998).
- [29] M. Gonzalez-Alonso, A. Pich and J. Prades, *Phys. Rev. D* **81** (2010) 074007; *D* **82** (2010) 04019.
- [30] D. Boito, M. Golterman, M. Jamin, K. Maltman and S. Peris, *Phys. Rev. D* **87** (2013) 094008.
- [31] C. Dominguez, L. Hernandez, K. Schilcher and H. Spiesberger, *JHEP* **03**, 053 (2015).
- [32] M. A. Shifman, A. I. Vainshtein, M. B. Voloshin and V. I. Zakharov, *Phys. Lett. B* **77**, 80 (1978).
- [33] V. A. Novikov, L. B. Okun, M. A. Shifman, A. I. Vainshtein, M.B. Voloshin and V.I. Zakharov, *Phys. Rep.* **41**, 1 (1978); *Phys. Lett. B* **67**, 409 (1977).
- [34] D. Arndt and C. R. Ji, *Phys. Rev. D* **60**, 094020 (1999).
- [35] T. Yamazaki *et al.* [CP-PACS], *Phys. Rev. D* **65**, 014501 (2002).
- [36] S. x. Qin, L. Chang, Y. x. Liu, C. D. Roberts and D. J. Wilson, *Phys. Rev. C* **85**, 035202 (2012).
- [37] Y. Kwon, M. Procura and W. Weise, *Phys. Rev. C* **78**, 055203 (2008).
- [38] S. Leupold, W. Peters and U. Mosel, *Nucl. Phys. A* **628**, 311 (1998).
- [39] T. Hatsuda and S. H. Lee, *Phys. Rev. C* **46**, no. 1, R34 (1992).
- [40] M. Neubert, *Phys. Rev. D* **45** (1992) 2451.
- [41] P. Ball, V. M. Braun and H. G. Dosch, *Phys. Rev. D* **48**, 2110-2120 (1993).
- [42] V. Belyaev, A. Khodjamirian and R. Ruckl, *Z. Phys. C* **60**, 349-356 (1993).
- [43] T. Huang, Z. H. Li and C. W. Luo, *Phys. Lett. B* **391**, 451-455 (1997).
- [44] Y. b. Dai, C. s. Huang, M. q. Huang, H. Y. Jin and C. Liu, *Phys. Rev. D* **58**, 094032 (1998).
- [45] S. V. Mikhailov and A. V. Radyushkin, *JETP Lett.* **43**, 712 (1986).
- [46] A. Grozin, *Int. J. Mod. Phys. A* **10**, 3497-3529 (1995).
- [47] A. P. Bakulev, A. V. Pimikov and N. G. Stefanis, *Phys. Rev. D* **79**, 093010 (2009).
- [48] R. C. Hsieh and H. n. Li, *Phys. Lett. B* **698**, 140-145 (2011).